Theory of electron spin echoes in solids

2002 J. Phys.: Condens. Matter 14 10349

(http://iopscience.iop.org/0953-8984/14/43/330)

INSTITUTE OF PHYSICS PUBLISHING JOURNAL OF PHYSICS: CONDENSED MATTER

J. Phys.: Condens. Matter **14** (2002) 10349–10365 PII: S0953-8984(02)37027-9

Theory of electron spin echoes in solids

N Ya Asadullina, T Ya Asadullin[1] and Ya Ya Asadullin

Kazan State Technical University, Department of General Physics, Karl Marx Street 10, Kazan 420111, Russia

E-mail: atimur@physics.kstu-kai.ru

Received 15 May 2002
Published 18 October 2002
Online at stacks.iop.org/JPhysCM/14/10349

Abstract

We propose modified Bloch equations (MBEs) with specific power-dependent relaxation and dispersion parameters characteristic for two-pulse excitation and when the magnetic dipole–dipole interactions in the electron spin system control the dephasing. We discriminate between the '*active*' (excited by both pulses) and '*passive*' (excited by the second pulse only) spins: it is shown that the 'active' spins participate in a new effect, an *active spin frequency modulation* effect giving rise to the power-dependent dispersion and multiple electron spin echoes (ESEs); the 'passive' spins contribute to the power-dependent relaxation. The MBEs are solved and a general expression for the two-pulse ESEs is obtained. Detailed numerical analysis of this expression gives results in good quantitative agreement with the recent experiments on the two-pulse ESEs at conventional low applied fields. The developed theory is applied also to high field ESEs, which are promising for future investigations. On the basis of published results it is deduced that the instantaneous diffusion mechanism is ineffective.

1. Introduction

The purpose of this paper is to explain recent experiments [1, 2] on the electron spin echoes (ESEs) in solids. In particular, the results on the power dependence of the irreversible phase relaxation rate $\Gamma = T_2^{-1}$ and its spectral properties [1], the existence of multiple echoes at high applied fields [2] and the interrelation between these effects and the so-called instantaneous diffusion (ID) effect [3] are of significant importance.

An important contribution to the phase relaxation in ESEs of solids is due to the dipole–dipole interaction of the paramagnetic centres. Because of the many-particle nature of the dipole–dipole interactions, satisfactory microscopic analysis of the relaxation and, hence, of the echo phenomenon in general is impossible.

[1] Author to whom any correspondence should be addressed.

For description of the transient phenomena in two-level ($S = 1/2$) systems excited by a resonant field $H_1(t) = 2H_{mw}\cos(\omega_1 t)$, the phenomenological Bloch equations are widely used. In the rotating reference frame (RRF) with frequency ω_1, these equations are

$$\begin{aligned} \dot{u} + \Delta v + \frac{u}{T_{2u}} &= 0, \\ \dot{v} - \Delta u - \chi\, w + \frac{v}{T_{2v}} &= 0, \\ \dot{w} + \chi\, v + \frac{(w - w_0)}{T_1} &= 0. \end{aligned} \tag{1}$$

Here u and v are the components of the transition dipole moment in phase and out of phase with $H_1(t)$; w is the population difference or, equivalently, the polarization with the equilibrium value w_0. (In magnetic resonance, alternatively, u, v and w are the components of the magnetization.) For electron spins $w_0 = \tanh(g\beta_e H_0/2k_B T)$, where g and β_e are the g-factor and the Bohr magneton of the electron respectively and H_0 is the applied magnetic field. In many cases, including EPR of solids, the resonance spectrum is inhomogeneously broadened and the resonance frequency ω of the spins is distributed as $f(\varepsilon = \omega - \omega_0)$ around the centre frequency $\omega_0 = \gamma H_0$, where γ is the gyromagnetic ratio. Then equations (1) refer to the generic homogeneous spin packet with frequency ω. Ordinary Bloch equations (OBEs) properly (1) include two constant phenomenological relaxation parameters, T_1 and $T_{2u} = T_{2v} = T_2 = \Gamma^{-1}$, the power-independent tuning parameter $\Delta = \omega - \omega_1$ and the induced Rabi frequency $\chi = \gamma H_{mw}$. Besides Δ, we introduce detuning of the driving field from the centre frequency $\Delta_0 = \omega_1 - \omega_0$. Obviously, $\varepsilon = \Delta + \Delta_0$.

Experiments on transient nutations (TNs), free induction decay (FID) and echoes in NMR [4], EPR [1, 2, 5, 6] and optics [7–10] of solids show that parameter T_2 and frequency ω are not constants but depend on the intensity of the excitation field. So, the Bloch equations (1) should be properly modified by taking into account the power dependences of ω (H_1) and $T_2(H_1)$.

A version of the modified Bloch equations (MBEs) was proposed in recent publications [11, 12] and used to describe experiments on TN and FID in EPR [4, 5] and applied to the theory of spectral hole burning (see also [13, 14]). In distinction to previous theories on MBE (see, for example, [15–17]), where the non-Bloch behaviour of the transient responses has been ascribed to the fluctuations of the resonance frequency ω_0 of the active centres and/or of the field source, in [11] the power dependence of ω and T_2 is directly attributed to the changes in the system of the active centres caused by the interaction with the coherent excitation field. It was known long ago [18, 19] that the power dependence of T_2 is different in equations for u and v components of equations (1). While there is a more or less satisfactory theory and expressions for T_{2u} [18, 19], the meaning of T_{2v} is not so clear. In [11, 12] the power dependence of T_{2v} was associated with the creation of the transverse components of the magnetization by the excitation field. From experiments on the ESE [1] it follows, however, that it is more realistic to refer this power dependence to the changes in the longitudinal component of the magnetization.

The next section is devoted to the analysis of the power-dependent variations of ω and T_2 introduced by the coherent excitation pulses in the inhomogeneously broadened system and their relation to the ID mechanism. In section 3 we solve the Bloch equations modified in such a way for a sequence of the two excitation pulses and obtain a general expression for the two-pulse ESEs. In section 4 this general expression is analysed numerically as a function of the various pulse parameters (the Rabi frequency χ, pulse length t_p, interval between the pulses τ), of the applied field H_0 and so on and the results of the calculations are compared

with the experimental data. A brief discussion of our results and results of other publications is given in section 5.

2. Power dependence of the MBE parameters and the ESE nonlinear mechanisms

The echo formation is a more complex and subtle phenomenon than the TN effect and/or FID each taken separately. This is due to the fact that the echo is a coherent nonlinear response and its formation, amplitude and decay properties strongly depend on the phase relations between the pulses. The correct accounting for these relations is the main task of any echo theory.

The nonlinear mechanisms of ESE consist of

(i) the *nonlinear excitation*,
(ii) the *nonlinear (intensity-dependent) dispersion* and, possibly,
(iii) the *nonlinear (intensity-dependent) damping* in the system of the active centres.

The nonlinear excitation mechanism (i) is connected with the terms $-\chi w$ and χv of equations (1) *nonlinear* in the excitation field. Unlike the polarization echoes in piezoelectric powders [20, 21], where the equation of motion for the elastic vibrations of the particle $s(t)$ contains both the strong *linear* piezoelectric force $\sim\beta E(t)$ (β is the piezoelectric constant, $E(t)$ is the excitation electric field) and the *nonlinear* electrostriction force $\sim E^2 s$, equations (1) do not contain the linear terms $\sim\chi \sim H_1(t)$.

The nonlinear dispersion mechanism (ii) is responsible for the multiple echoes and in the system of dipoles is due to the demagnetizing field [4]. This mechanism is considered and applied to the echo formation in the strongly homogeneous system (nuclear spins in solid ^{3}He), where the space inhomogeneity of the applied field $\boldsymbol{H}_0$ is created artificially by applying a uniform field gradient $\boldsymbol{G}$, in [4]. As a result, a sinusoidal modulation of the magnetization along the gradient direction appears at the end of the second pulse. The demagnetizing field corresponding to this magnetization generates a spatially sinusoidally modulated Larmor frequency which acts on the transverse component $M_+ = u + \mathrm{i}v$. So, $M_+(t)$ after the pulses consists of the infinite spatial Fourier components $M_+(\boldsymbol{k}, t)$. It is shown [4] that at times $t = n\tau$ ($n = 2, 3, \ldots$) where τ is the time interval between the pulses, $M_+(t)$ becomes uniform ($\boldsymbol{k} = 0$) giving rise to the multiple echoes at those times.

In the case of the inhomogeneously broadened systems [1, 2] where the magnetization all the time remains spatially uniform, the demagnetizing field works in a somewhat different way and requires a special consideration. For this purpose, it is instructive to consider, even if schematically, the time evolution of the spin system microscopically.

We take the spin Hamiltonian in the RRF of the form

$$H_0 = \hbar \sum_k \Delta_k S_{kz} + \hbar \sum_{i \neq k} A_{ik} S_{iz} S_{kz} \tag{2}$$

where $A_{ik} = A_{ik}(r_{ik}, \theta_{ik})$ is the usual expression of the dipole–dipole interaction and $\Delta_k = \omega_k - \omega_1$ is the resonance offset. During the short and strong mw pulses, the Hamiltonian is

$$H = H_0 + H_p \approx H_p = \hbar \chi_p \sum_k S_{kx} \tag{3}$$

where χ_p is the Rabi frequency of the pulse.

The transverse component of the magnetization of a particular spin packet in the RRF at time t is given by

$$M_{j+}(t) = g\beta_e \langle S_{j+}(t) \rangle = g\beta_e \mathrm{Tr}\,[\rho(t) S_{j+}] \tag{4}$$

where the density operator

$$\rho(t) = R(t)\rho(0)R^{-1}(t) \tag{5}$$

describes the evolution of the spin system during the echo-formation process. In the high temperature approximation

$$\rho(0) \approx 1 - \frac{\hbar\omega_0}{k_B T}\sum_k S_{kz} \to -\frac{\hbar\omega_0}{k_B T}\sum_k S_{kz}. \tag{6}$$

The evolution operator for the two-pulse echo sequence is

$$\begin{aligned} &R(t) = R_{f2}(t-\tau)R_{p2}R_{f1}(\tau)R_{p1} \\ &R_{pi} = \exp\{-\mathrm{i}\hbar^{-1}H_i t_i\} = \exp\left\{-\mathrm{i}\chi_i t_i \sum_k S_{kx}\right\} = \exp\left\{-\mathrm{i}\Theta_i \sum_k S_{kx}\right\} \\ &R_{fi}(t) = \exp\{-\mathrm{i}\hbar^{-1}H_0 t\}. \end{aligned} \tag{7}$$

From equation (2) one can see that the equilibrium demagnetizing field operator is $H_d \sim \sum_i A_{ik}S_{iz}$. Equations (5) and (7) after the first pulse of flip angle $\Theta_1 = \chi_1 t_1$ give

$$S_{kz}(t_1) = S_{kz}\cos\Theta_1 - S_{ky}\sin\Theta_1 \tag{8}$$

so the demagnetizing field for the free precession after the pulse is $H_d(\tau) \sim \sum_i A_{ik}S_{iz}\cos\Theta_1$. Replacing in equation (2) S_{iz} by $S_{iz}\cos\Theta_1$, from equation (7) one obtains for the free precession

$$\begin{aligned} &S_{kz}(t_1,\tau) = S_{kz}\cos\Theta_1 - \sin\Theta_1(S_{ky}\cos\psi_{1k} - S_{kx}\sin\psi_{1k}) \\ &\psi_{1k} = (\Delta_k + \cos\Theta_1 \sum_{i\neq k} A_{ki}S_{iz})\tau. \end{aligned} \tag{9}$$

It is seen from (9) that the first pulse simply uniformly shifts the resonance spectrum by $\delta\omega^{(1)} = (1-\cos\Theta_1)\sum_i A_{ik}\langle S_{iz}\rangle$. A similar consideration holds for the effect on the demagnetizing field by the second pulse. The final expression for $\rho(t) \sim \sum_k S_{kz}(t_1, \tau, t_2, t-\tau)$ at time t from the beginning of the two-pulse sequence is given by

$$\begin{aligned} &S_{kz}(t_1,\tau,t_2,t-\tau) = a_{kz}S_{kz} + a_{k-}S_{k+}\mathrm{e}^{-\mathrm{i}\varpi_k(t-\tau)} + a_{k+}S_{k-}\mathrm{e}^{\mathrm{i}\varpi_k(t-\tau)} \\ &a_{kz} = \cos\Theta_1\cos\Theta_2 - \sin\Theta_1\sin\Theta_2\cos\phi_k \\ &a_{k-} = -\frac{\mathrm{i}}{2}[\cos\Theta_1\sin\Theta_2 + \sin\Theta_1\cos^2(\Theta_2/2)\mathrm{e}^{\mathrm{i}\phi_k} - \sin\Theta_1\sin^2(\Theta_2/2)\mathrm{e}^{-\mathrm{i}\phi_k}]; \quad a_{k+} = a_{k-}^* \\ &\phi_k = \left(\Delta_k + 2\cos\Theta_1\cos\Theta_2\sum_{i\neq k}A_{ki}S_{iz}\right)\tau \\ &\varpi_k = \Delta_k + b_{kc}\cos\Delta_k\tau + b_{ks}\sin\Delta_k\tau + b_{k0}. \end{aligned} \tag{10}$$

In obtaining the expression for ϕ_k we neglect terms $\sim S_{iy}$. Furthermore, ϖ_k represents the effect of the successive two-pulse excitation on the transition frequency of a kth spin packet: b_{k0} contains terms that simply uniformly shift the resonance frequency and sums of terms that are effectively averaged to zero; terms $\sim b_{kc}$ and $\sim b_{ks}$ describe the desired periodically modulated contributions to the transition frequency and actually represent the nonlinear dispersion mechanism; we emphasize their locality in the frequency domain, that is they depend on the frequency Δ_k (and phase $\Delta_k\tau$) of the same spin packet under consideration only. In the important particular case of $\Theta_1 = \pi/2$ one has $b_{ks} = 0$ and

$$b_{kc}(\Theta_1 = \pi/2) = -\sin\Theta_1\sin\Theta_2\sum_{i\neq k}A_{ki}\langle S_{iz}\rangle. \tag{11}$$

As usual [4, 20], the Fourier expansion

$$\exp[\mathrm{i}(t-\tau)b_{kc}\cos\Delta_k\tau] = \sum_{n=-\infty}^{\infty}\mathrm{i}^n J_n[(t-\tau)b_{kc}]\exp(\mathrm{i}n\Delta_k\tau) \tag{12}$$

with the Bessel functions $J_n(x)$ as the Fourier coefficients leads, after the insertion of $\rho(t)$ into (4) and integration over the inhomogeneous distribution of the spin packets $g(\Delta)$, to the multiple echoes at times $t = n\tau$ ($n = 2, 3, \ldots$).

From equation (4) one sees that a_{kz}-term in (10) does not contribute to the transverse magnetization. It is important for the three-pulse (stimulated) echoes not considered in this paper.

The intensity-dependent damping (iii) due to the dipole–dipole interactions cannot be described in the way given above for the nonlinear dispersion. Hence, we shall confine ourselves to rather a qualitative discussion based on the experimental results [1].

Inasmuch as pulse duration $t_i \ll T_2$ [1, 2], during the pulses one can with sufficient accuracy neglect the relaxation terms in equations (1). Thus, the damping described by the parameter T_{2u} is of no any importance in this approximation, as the free precession of both u and v is governed by $\Gamma = T_{2v}^{-1}(\chi)$ formed during the pulse. The decay rate $\Gamma^{(1)}$ after the first pulse can be written as

$$\Gamma^{(1)} = \Gamma_0 + \Gamma^{(1)}(\chi_1) \tag{13}$$

where Γ_0 represents the power-independent damping due to the interaction of the coherently excited spins with the thermally excited ones. Its temperature dependence can be approximated by [22]

$$\Gamma_0 = \Gamma_{00}(1 - w_0^2)^{1/2}. \tag{14}$$

The second term in (13) describes the power-dependent damping due to the interaction among the coherently excited spins. For spins coherently excited by a short duration pulse this term is effectively equal to zero at any time if the space distribution of the active centres is uniform; then one has $\Gamma^{(1)} = \Gamma_0$.

We divide the spins excited by the second pulse into two groups with different phase properties: $n_2 = n_{2ac} + n_{2pas}$. Here n_{2ac} represents the echo-forming ('*active*') spins excited by both the pulses and the phase properties of which are described by formulae (10). There arose the question of whether there is a nonlinear damping mechanism similar to the nonlinear dispersion given by expression (10) for ϖ_k. In our opinion [11, 23], such a mechanism exists, though this existence depends on the unclear role of the 'active' spins in the nonlinear damping. Supposedly, however, as in the case of the polarization echoes in powders [21] and cyclotron echoes in plasmas [24], it is of lesser importance than mechanisms (i) and (ii): for the pulses of low intensity its contribution is small; at high powers the echo amplitude is dominated by the increasing damping. So, below it is imagined that the spins of n_{2ac} do not contribute to the power-dependent damping and this mechanism is excluded from the consideration.

Group n_{2pas} consists of the new spins excited during the second pulse and described by equation (8) with index 2 instead of 1 there. It is obvious that these '*passive*' spins do not participate directly in the echo-formation process. They contribute, however, to the power-dependent damping in the system of the 'active' spins. From experiments [1] it follows that this contribution is proportional to the change in the polarization $\delta w(t_2) = w_0 - \langle w_{pas}(t_2)\rangle$ where $\langle w_{pas}(t_2)\rangle$ is the average polarization of the 'passive' spins at the end of the second pulse. Hence, decay rate $\Gamma^{(2)}$ after the second pulse is

$$\Gamma^{(2)} = \Gamma_0 + \Gamma(\chi_2) = \Gamma_0 + a_\Gamma \delta w(t_2). \tag{15}$$

Note that the given division of the *resonant* spins into the two groups has nothing in common with the known division [3] into the A (resonant) and B (nonresonant) spins where the A spins are responsible for the ID effect while the B spins lead to the spectral diffusion (SD) effect.

3. Modified Bloch equation theory of ESE

Here we develop a simple theory of ESE in solids based on the MBEs which take into account the results of mechanisms (ii) and (iii) of the preceding section. The solution of (1) at the end of the first pulse is

$$\begin{aligned} &u(t_1) = w_0\chi_1(\varepsilon-\Delta_0)(1-\cos\Phi_1)/\Omega_1^2 \\ &v(t_1) = -w_0\chi_1\sin\Phi_1/\Omega_1 \\ &w(t_1) = w_0[(\varepsilon-\Delta_0)^2+\chi_1^2\cos\Phi_1]/\Omega_1^2 \\ &\Omega_1^2 = [(\varepsilon-\Delta_0)^2+\chi_1^2] \quad \Phi_1 = \Omega_1 t_1. \end{aligned} \tag{16}$$

For the free precession between the pulses from equations (1) with parameters $T_{2u} = T_{2v} = \Gamma_0^{-1}$ and $\Delta = \varepsilon - \Delta_0 + \delta\omega^{(1)}$ we have

$$\begin{aligned} &u(t_1,\tau) = [u(t_1)\cos\psi_1 - v(t_1)\sin\psi_1]\mathrm{e}^{-\Gamma_0\tau} \\ &v(t_1,\tau) = [v(t_1)\cos\psi_1 + u(t_1)\sin\psi_1]\mathrm{e}^{-\Gamma_0\tau} \\ &w(t_1,\tau) = w(t_1)\ldots\psi_1 = (\varepsilon-\Delta_0+\delta\omega^{(1)})\tau \\ &\delta\omega^{(1)} = a_\omega(w_0-\langle w(t_1)\rangle) \quad \langle w(t_1)\rangle = \int_{-\infty}^{\infty} w(t_1)f(\varepsilon)\,\mathrm{d}\varepsilon. \end{aligned} \tag{17}$$

For $\tau \ll T_1$ here the longitudinal relaxation is neglected. Parameter $a_\omega \sim \sum_i A_{ik}$.

The solution of equations (1) for the 'active' spins at the end of the second pulse is

$$\begin{aligned} u(t_1,\tau,t_2) &= \Omega_2^{-2}\{u(t_1,\tau)[\chi_2^2\cos^2\varphi + (\chi_2^2\sin^2\varphi + (\varepsilon-\Delta_0)^2)\cos\Phi_2] \\ &\quad + v(t_1,\tau)[\chi_2^2\sin\varphi\cos\varphi(1-\cos\Phi_2) - (\varepsilon-\Delta_0)\Omega_2\sin\Phi_2] \\ &\quad + w(t_1,\tau)\chi_2[\Omega_2\sin\varphi\sin\Phi_2 + (\varepsilon-\Delta_0)\cos\varphi(1-\cos\Phi_2)]\} \\ v(t_1,\tau,t_2) &= \Omega_2^{-2}\{u(t_1,\tau)[\chi_2^2\sin\varphi\cos\varphi(1-\cos\Phi_2) + (\varepsilon-\Delta_0)\Omega_2\sin\Phi_2] \\ &\quad + v(t_1,\tau)[\chi_2^2\sin^2\varphi + (\chi_2^2\cos^2\varphi + (\varepsilon-\Delta_0)^2)\cos\Phi_2] \\ &\quad + w(t_1,\tau)\chi_2[-\Omega_2\cos\varphi\sin\Phi_2 + (\varepsilon-\Delta_0)\sin\varphi(1-\cos\Phi_2)]\} \\ w(t_1,\tau,t_2) &= \Omega_2^{-2}\{u(t_1,\tau)\chi_2[(\varepsilon-\Delta_0)\cos\varphi(1-\cos\Phi_2) - \Omega_2\sin\varphi\sin\Phi_2] \\ &\quad + v(t_1,\tau)\chi_2[(\varepsilon-\Delta_0)\sin\varphi(1-\cos\Phi_2) + \Omega_2\cos\varphi\sin\Phi_2] \\ &\quad + w(t_1,\tau)[(\varepsilon-\Delta_0)^2+\chi_2^2\cos\Phi_2]\} \\ &= c_0 + c_1\mathrm{e}^{-\Gamma_0\tau}\cos[(\varepsilon-\Delta_0)\tau-\varphi] + c_2\mathrm{e}^{-\Gamma_0\tau}\sin[(\varepsilon-\Delta_0)\tau-\varphi] \\ c_0 &= w_0(\Omega_1\Omega_2)^{-2}[(\varepsilon-\Delta_0)^2+\chi_1^2\cos\Phi_1][(\varepsilon-\Delta_0)^2+\chi_2^2\cos\Phi_2] \\ c_1 &= -w_0\frac{\chi_1\chi_2}{\Omega_1\Omega_2}\mathrm{e}^{-\Gamma_0\tau}\left[\sin\Phi_1\sin\Phi_2 - \frac{(\varepsilon-\Delta_0)^2}{\Omega_1\Omega_2}(1-\cos\Phi_1)(1-\cos\Phi_2)\right] \\ c_2 &= w_0\frac{\chi_1\chi_2}{\Omega_1\Omega_2}\mathrm{e}^{-\Gamma_0\tau}\left[\frac{(\varepsilon-\Delta_0)}{\Omega_2}\sin\Phi_1(1-\cos\Phi_2) + \frac{(\varepsilon-\Delta_0)}{\Omega_1}(1-\cos\Phi_1)\sin\Phi_2\right] \\ \Omega_2^2 &= (\varepsilon-\Delta_0)^2+\chi_2^2 \quad \Phi_2 = \Omega_2 t_2. \end{aligned} \tag{18}$$

Here $\varphi = \varphi_2 - \varphi_1$ is the phase difference between the pulses. Small and, hence, insufficient uniform contributions to the resonance frequency are neglected in (18). For free evolution of the 'active' spins after the second pulse in MBEs (1) we have parameters $\Gamma^{(2)}$ and $\Delta = \varepsilon - \Delta_0 + \delta\omega^{(2)}$

and solution

$$\begin{aligned}
&u(t_1,\tau,t_2,t) = [u(t_1,\tau,t_2)\cos\psi_2 - v(t_1,\tau,t_2)\sin\psi_2]\mathrm{e}^{-\Gamma^{(2)}(t-\tau)}\\
&v(t_1,\tau,t_2,t) = [v(t_1,\tau,t_2)\cos\psi_2 + u(t_1,\tau,t_2)\sin\psi_2]\mathrm{e}^{-\Gamma^{(2)}(t-\tau)}\\
&w(t_1,\tau,t_2,t) = w(t_1,\tau,t_2)\\
&\psi_2 = (\varepsilon - \Delta_0 + \delta\omega^{(2)})(t-\tau)\\
&\delta\omega^{(2)} = a_\omega^{ac}(w_0 - w(t_1,\tau,t_2)) + a_\omega^{pas}(w_0 - \langle w_{pas}(t_2)\rangle)\\
&\Gamma^{(2)} = \Gamma_0 + a_\Gamma\delta w(t_2) = \Gamma_0 + a_\Gamma(w_0 - \langle w_{pas}(t_2)\rangle)\\
&\langle w_{pas}(t_2)\rangle = \int_{-\infty}^{\infty} w_{pas}(t_2)\,f(\varepsilon)\,\mathrm{d}\varepsilon\\
&w_{pas}(t_2) = w_0[(\varepsilon-\Delta_0)^2 + \chi_2^2\cos\Phi_2]/\,\Omega_2^2.
\end{aligned} \tag{19}$$

In accord with the results of mechanism (ii) of the preceding section, $\delta\omega^{(2)}$ and, hence, ψ_2 contain the desired periodically modulated contribution to the resonance frequency from the 'active' spins while term $\sim a_\omega^{pas}$ leads to the uniform shift. Furthermore, term $\sim a_\Gamma$ in (19) describes the important [1] power-dependent contribution to the decay rate from the 'passive' spins excited by the second pulse (see equation (15) above).

Observed echoes are given by

$$V(t_1,\tau,t_2,t,\chi_1,\chi_2,\Delta_0,\varphi) \sim \int_{-\infty}^{\infty}[u^2(t_1,\tau,t_2,t) + v^2(t_1,\tau,t_2,t)]^{1/2}\,f(\varepsilon)\,\mathrm{d}\varepsilon \tag{20}$$

and can be examined as a function of any of the arguments shown in this formula. As a first step, we may apply expansion (12) to $\cos\psi_2$ and $\sin\psi_2$. The substitution into $u(t_1,\tau,t_2,t)$ and $v(t_1,\tau,t_2,t)$ and the integration over ε (20) leads to the echoes at times $t = n\tau$ ($n = 2, 3, 4\ldots$). However, the general expression obtained in this way is a very complex expression and the analytic evaluation of the echo properties presents large difficulties. On the other hand, $V(t_1,\tau,t_2,t,\chi_1,\chi_2,\Delta_0,\varphi)$ can be easily examined numerically and successfully compared with the experimental results.

4. Numerical calculations

4.1. Low field ESE

Our calculations are mainly connected with the decay properties of the echo [1]. As seen from expression (20), the calculations need a specific expression for the inhomogeneous distribution $f(\varepsilon)$. Usually it is presumed as a Gaussian

$$f(\varepsilon) = (2\pi)^{-1/2}\sigma^{-1}\exp[-(\varepsilon-\varepsilon_0)^2/2\sigma^2] \tag{21}$$

though the distribution experimentally [1] obtained and used below is not symmetrical (full curve in figure 1). Because of low values of the polarization in experiments [1] ($w_0 = 0.033\,687$ at 4.2 K) somewhat cumbersome expressions (16)–(19) are simplified. Indeed, $\delta\omega^{(2)}$ in (19) is negligibly small, the nonlinear dispersion mechanism is insufficient and, hence, multiple echoes at times $t = 3\tau, 4\tau, \ldots$ are not observable.

Moreover, in (14) we have $\Gamma_0 \approx \Gamma_{00}$. Then from formulae (16)–(19) it follows that the decay function of the 2τ echo is given by

$$\begin{aligned}
&V(t=2\tau) = V_0\exp(-\Gamma_{00}\tau - \Gamma^{(2)}\tau) = V_0\exp(-2\Gamma_{eff}\tau)\\
&\Gamma_{eff} = \Gamma_{00} + \frac{a_\Gamma}{2}(w_0 - \langle w_{pas}(t_2)\rangle).
\end{aligned} \tag{22}$$

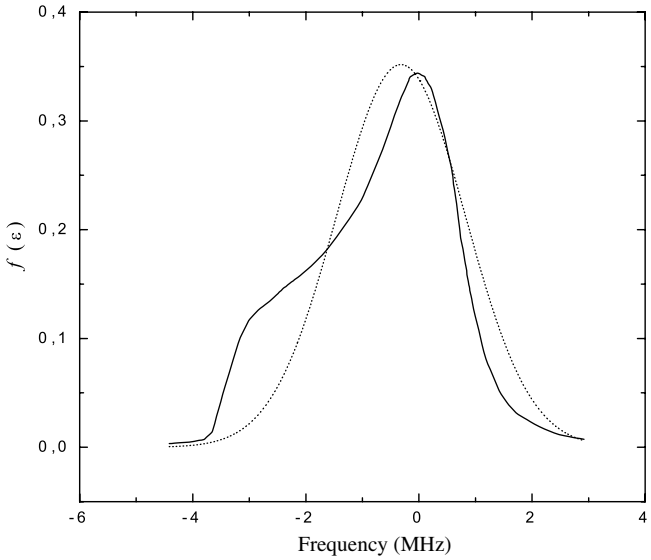

Figure 1. Inhomogeneous distribution of the spins $f(\varepsilon)$. The full curve is the experimental result [1] and the dotted curve is given by equation (21).

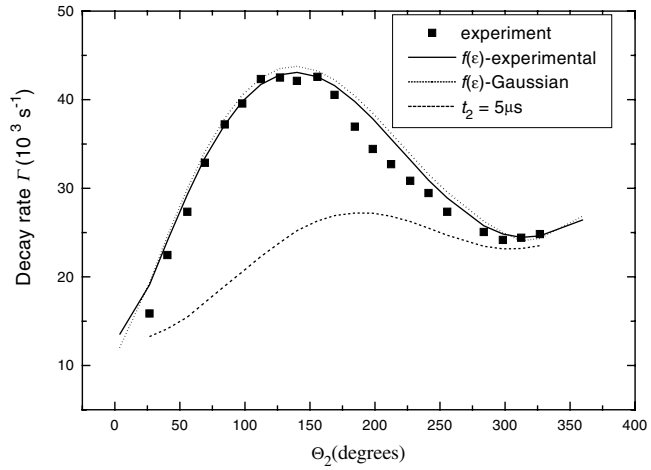

Figure 2. Echo decay rate Γ as a function of the second pulse area Θ_2. Dots are the experimental values of Γ [1]; the full curve and the dotted curve are calculated from equation (20) with the experimental and the Gaussian distributions $f(\varepsilon)$ respectively. For all three cases $\chi_2 = 2\pi \times 200$ kHz. The dashed curve is for $t_2 = 5$ μs and varying χ_2.

That is, the echo decay is strongly exponential, but with the intensity-dependent decay rate $\Gamma = \Gamma_{eff}$, in accordance with experiment [1]. Dots in figure 2 show the experimental values of Γ as a function of the tilt angle $\Theta_2 = \chi_2 t_2$ obtained for constant value $\chi_2 = \chi_1 = 2\pi \times 200$ kHz, $t_1 = 1.667$ μs and varying t_2 [1]. The full curve depicts the same dependence obtained from expression (20) as $V(\tau)$ with the use of the experimental function $f(\varepsilon)$ given in figure 1. To obtain this result, besides the above parameters the following values of the parameters were used: $\Gamma_{00} = 12.5 \times 10^3$ s^{-1}, $a_\Gamma = 6.4 \times 10^6$ s^{-1}.

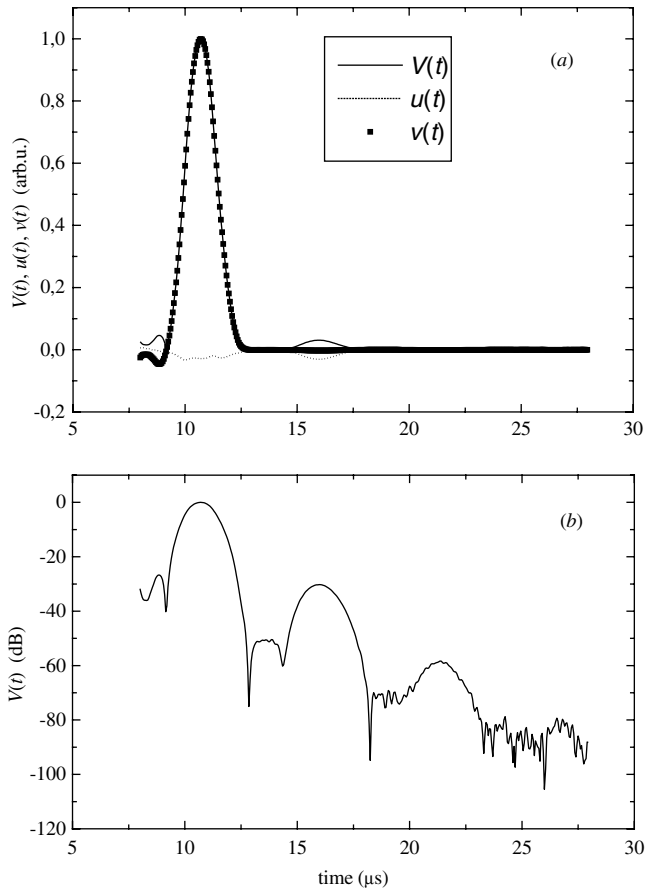

Figure 3. (a) Contributions of the u and v components to the multiple echoes; (b) the multiple echoes in dB.

We have repeated the same calculations with $f(\varepsilon)$ given by Gaussian (21) with the parameters $\varepsilon_0 = 2 \times 10^6\ \mathrm{s}^{-1}$, $\sigma = 7.14 \times 10^6\ \mathrm{s}^{-1}$ (see the dotted curve in figure 1) and $a_\Gamma = 6.5 \times 10^6\ \mathrm{s}^{-1}$; the result is given by the dotted curve in figure 2. Finally, we have calculated directly Γ_{eff} as the function of Θ_2 varying t_2 with the use of the experimental function $f(\varepsilon)$; the result exactly coincides with the full curve, so it is not shown in figure 2. All the results below in this section, unless otherwise noted, are obtained with the use of the experimental function $f(\varepsilon)$ only.

Note that $\Gamma(\Theta_2)$ can be examined also as a function of χ_2 with a given value of t_2; an example for $t_2 = 5\ \mu$s when $\Theta_2 = 2\pi$ for $\chi_2 = 2\pi \times 200$ kHz [1] is shown by the dashed curve in figure 2. Since Γ_{eff} depends on χ_2 not only through Θ_2 (see (19) and (22)), the two cases, $\Gamma(\Theta_2, t_2)$ and $\Gamma(\Theta_2, \chi_2)$, give different dependences for $\Gamma(\Theta_2)$ on Θ_2.

The upper limit of parameter a_ω^{ac} in (19) representing the demagnetizing field and responsible for the multiple echoes can be estimated as follows. Figure 3(a) shows the multiple echoes $V(t)$ (full curve) and the contributions of the $u(t)$ (dotted curve) and $v(t)$ (squares) components obtained with the following values of parameters: $\chi_1 = \chi_2 = 2\pi \times 200$ kHz, $\tau = 5\ \mu$s, $t_1 = t_2 = 1.25\ \mu$s ($\Theta_1 = \Theta_2 = \pi/2$), $\Gamma_{00} = 12.5 \times 10^3\ \mathrm{s}^{-1}$, $a_\Gamma = 6.4 \times 10^6\ \mathrm{s}^{-1}$, and $a_\omega^{ac} = 3 \times 10^5\ \mathrm{s}^{-1}$. In figure 3(b) the same result is given in a semilogarithmic scale. It is

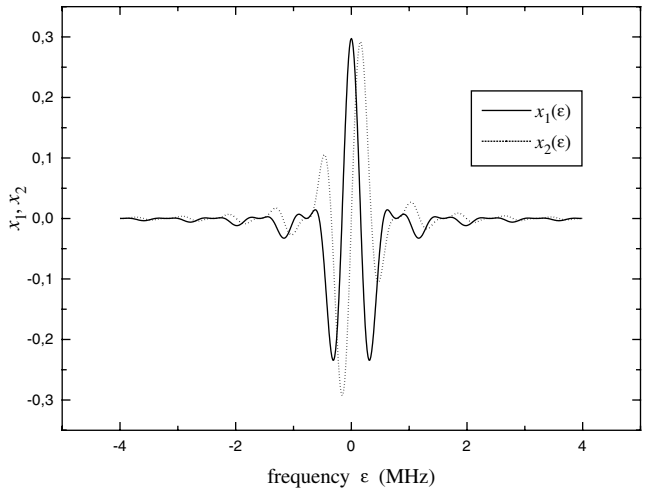

Figure 4. The frequency dependence of the characteristic parameters x_1 and x_2 of the multiple echoes (arguments of the Bessel functions) at low values of the applied field.

seen that the second echo is lower by 29 dB than the first echo which in the given conditions (t_1, t_2 and $\tau \ll T_2$) has really a maximal value. Because experimentally the signal decay is observed over a range of ≈30 dB [5], we conclude that $3 \times 10^5\ \mathrm{s}^{-1}$ represents the upper limit of a_ω^{ac} in [1]. The first echo and the third echo, poorly seen in figure 3(a), are due to $v(t)$ while the second echo is formed by $u(t)$.

The characteristic parameters which govern the echo pattern and, in particular, are responsible for the multiple echoes are the arguments of the Bessel functions $J_n(x)$ in equation (12) taken, say, at $t - \tau = \tau = T_2$. From equations (18) and (19) it follows that the arguments are $x_1 = a_\omega^{ac}(t-\tau)c_1$ and $x_2 = a_\omega^{ac}(t-\tau)c_2$. Note that in the homogeneously broadened system [4] $x_1 \sim c_1$ is the frequency-independent parameter (in [4] $x_1 \approx 20 \gg 1$) and $c_2 = 0$. In our case of the strongly inhomogeneous system x_1 and x_2 are frequency dependent, as seen from equations (18) and (19) and shown in figure 4 for $w_0 = 0.033\,687$, $\chi_1 = \chi_2 = 2\pi \times 200$ kHz, $\Theta_1 = \Theta_2 = \pi/2$, $T_2^{-1} = \Gamma_{00} = 12.5 \times 10^3\ \mathrm{s}^{-1}$ and $a_\omega^{ac} = 3 \times 10^5\ \mathrm{s}^{-1}$. Note that x_1 is symmetric and x_2 is asymmetric in ε; both the functions undergo fast changes in the narrow central part of the inhomogeneous distribution $f(\varepsilon)$ from $|x| \approx 0.3$ to zero; as a consequence of the small effective values of x_1 and x_2, the multiple echoes are not observable.

The authors of [1] also investigate how different spin packets within the inhomogeneous distribution contribute to the echo decay. For this purpose, the dependence of the decay rate on the spectral position of the spins was examined by looking at the ESE decay after the same $\Theta_1 = \Theta_2 = 2\pi/3 (\chi_1 = \chi_2 = 2\pi \times 120\,\mathrm{kHz})$ pulse sequence for different values of H_0, i.e., of the detuning $\Delta_0 = \omega_1 - \omega_0$. Symbols in figure 5 show the experimentally observed decay picture for three values of the detuning while the full curves are obtained from the present theory with the parameters $\Gamma_{00} = 9.9 \times 10^3\ \mathrm{s}^{-1}$, $a_\Gamma = 6 \times 10^6\ \mathrm{s}^{-1}$. The theoretical values of the decay rate, $\Gamma(\Delta H_0 = 0) = 27.5 \times 10^3\ \mathrm{s}^{-1}$, $\Gamma(\Delta H_0 = -0.5\ \mathrm{Oe}) = 20.6 \times 10^3\ \mathrm{s}^{-1}$ and $\Gamma(\Delta H_0 = +0.5\ \mathrm{Oe}) = 13.38 \times 10^3\ \mathrm{s}^{-1}$, are in good agreement with the experimental results $(26 \pm 1) \times 10^3\ \mathrm{s}^{-1}$, $(21 \pm 1) \times 10^3\ \mathrm{s}^{-1}$ and $(12.8 \pm 0.5) \times 10^3\ \mathrm{s}^{-1}$, respectively. We also obtain results very similar to those shown in figure 5 using, besides the above parameters, the above-mentioned Gaussian distribution.

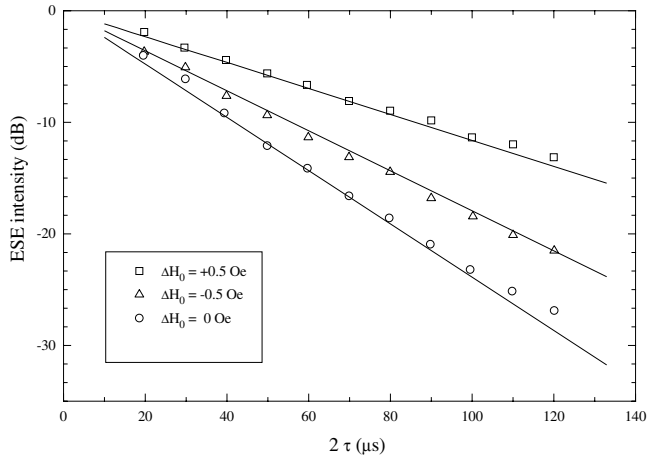

Figure 5. Echo decay curves for the same two-pulse sequence ($\Theta_1 = \Theta_2 = 120°$) at three different values of the detuning ΔH_0 from the resonance condition: $\Delta H_0 = 0$ Oe (circles), $\Delta H_0 = -0.5$ Oe (triangles) and $\Delta H_0 = +0.5$ Oe (squares). Symbols are the experimental results [1] and the full lines are from the present theory.

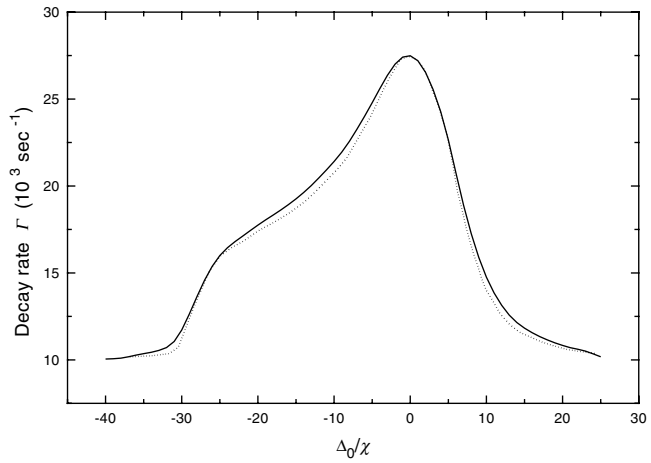

Figure 6. The echo decay rate Γ (full curve) versus detuning Δ_0, expressed in units of the Rabi frequency $\chi = 2\pi \times 120$ kHz. The dotted curve is the inhomogeneous distribution of the spins $f(\varepsilon)$ (see figure 1).

Figure 6 shows the echo decay rate $\Gamma = \Gamma_{eff}$ (full curve) versus detuning Δ_0, investigated in [1] as well. Parameters used in obtaining this figure are the same as for figure 5. One sees that this dependence $\Gamma(\Delta_0)$ is quite similar to the shape of the inhomogeneous distribution of the spins $f(\varepsilon)$ also shown by the dotted curve, in agreement with the experiment and theoretical analysis in [1].

4.2. High field ESEs

The investigations of ESE at high applied fields and low temperatures where $w_0 \approx 1$ [2] are very promising. In this case the nonlinear dispersion $\delta\omega^{(2)}$ is not negligible and may

affect the echo behaviour; in particular, the echo decay can be not pure exponential. Also, besides the dipole–dipole term (14), a contribution to the power-independent decay rate at high fields increasing with temperature gives the spin–lattice interaction. We approximate the total power-dependent decay rate after the second pulse $\Gamma_t^{(2)}$ by

$$\Gamma_t^{(2)} = \Gamma_{00}(1 - w_0^2)^{1/2} + \Gamma_{l0}(1 - w_0^2)/w_0 + a_\Gamma(w_0 - \langle w_{pas}(t_2)\rangle) \tag{23}$$

where Γ_{l0} refers to the spin–lattice interaction.

One of the results of [2] is the observation of a sequence of four two-pulse echoes. Figure 7 is an attempt to repeat this result with the parameters that presumably have been used in experiments [2], $w_0 = 0.998$ ($T = 4.2$ K, $H_0 = 215$ kOe), $\chi_1 = \chi_2 = (\pi/2) \times 10^7$ Hz and $\Theta_1 = \Theta_2 = \pi/2$, and with the following parameters of the present theory: $\Gamma_{00} = 3 \times 10^5$ s^{-1}, $\Gamma_{l0} = 6 \times 10^6$ s^{-1}, $a_\Gamma = 1 \times 10^6$ s^{-1}, $a_\omega^{ac} = 2 \times 10^6$ s^{-1} and $\tau = 0.2$ μs. The unknown inhomogeneous distribution is taken as Gaussian (21) with $\varepsilon_0 = 0$ and $\sigma = 1 \times 10^8$ s^{-1}.

It is seen from figure 7(a) that the first echo is due mainly to the $v(t)$ component, the secondary echo is formed by both components and the third echo is due mainly to the $u(t)$ component of the magnetization. Note, however, that the contributions of the components to the secondary echoes complicatedly depend on the above parameters. Also, it is worth noting that the fourth echo is less by 26 dB than the first one.

We should note that, in distinction to the low field echoes, at high fields the calculated echo decay is not exponential and this is the consequence of the significant nonlinear dispersion $\delta\omega^{(2)}$. Figure 8 shows calculated decay behaviour for the first (2τ) and second (3τ) echoes for 4.2 K. Only for larger values of τ (at the 'tail') does the decay becomes more or less exponential. The influence of the nonlinear dispersion decreases with the increasing temperature and at higher temperatures $T > 7$ K the decaying part is quite exponential. Figure 8 and other results below are calculated with the same parameters given above but $\sigma = 1 \times 10^7$ s^{-1}.

The measured memory decay rate of the high field echoes strongly depends on temperature, as shown by symbols in figure 9 for another sample [2]. Again, due to the nonlinear dispersion, the calculated decay rate Γ (full curve in figure 9) at low temperatures is not equal to Γ_{eff} (dotted curve in figure 9) given by

$$\Gamma_{eff} = \Gamma_{00}(1 - w_0^2)^{1/2} + \Gamma_{l0}(1 - w_0^2)/w_0 + \frac{a_\Gamma}{2}(w_0 - \langle w_{pas}(t_2)\rangle). \tag{24}$$

Really the nonlinear dispersion works to increase the memory time T_2. At higher temperatures $T > 7$ K where its effectiveness is lowered, $\Gamma(T)$ and $\Gamma_{eff}(T)$ merge as is seen from the figure.

In conclusion, we shall touch briefly on the characteristic parameters x_1 and x_2, responsible for the multiple echoes, at high applied fields. The calculations similar to those performed in the preceding subsection show that here we have the frequency dependence essentially of the same form as shown in figure 4. In this case, however, x_1 and x_2 span a ten times (for $T = 4.2$ K) broader frequency interval and their limiting values are larger ($\approx$15) than at low fields. Nevertheless, because of the fast variations, their effectiveness is less than in the case of the homogeneous systems where x_1 is independent of ε [4]. It is obvious from figure 4 that parameter x_1 symmetric in ε is more important for the multiple echoes than x_2.

5. Discussion

5.1. Low field ESE

The experimental results of figures 2, 5 and 6 are theoretically discussed in [1] as well, and good agreement similar to our calculations in those figures is achieved. The theoretical consideration

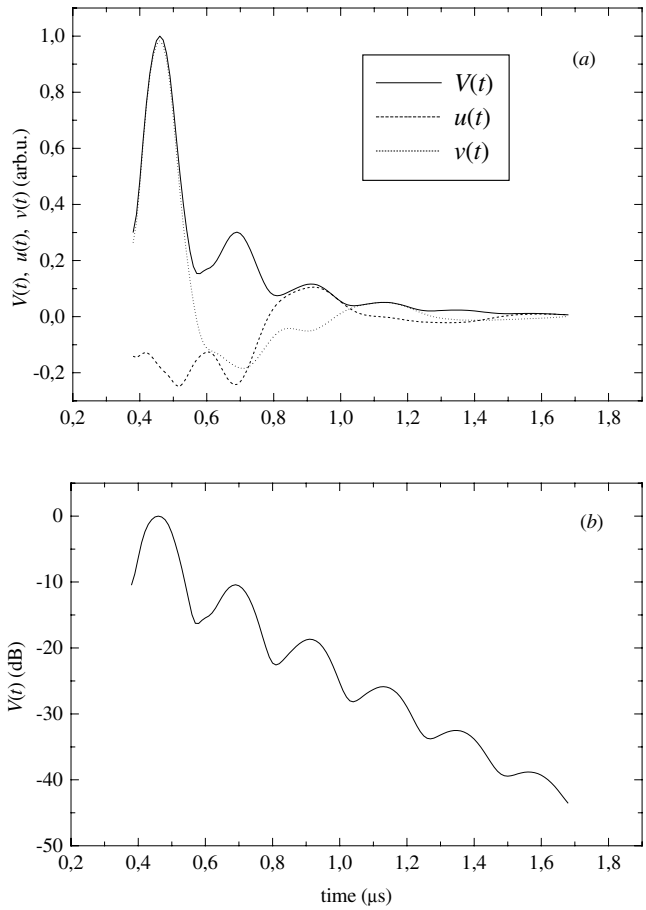

Figure 7. (a) Contributions of the u and v components to the high field multiple echoes; (b) the multiple echoes in dB.

in [1] is based on the ID mechanism. By definition [3], the ID effect consists in the following: a short rf pulse flips the A spins which causes a rapid (instantaneous) unbalance of transition frequencies of the B spins (and of the A spins as well). The influence on the motion of the A spins destructive in its nature introduced by a rapid B-spin reaction to this unbalance is termed the ID effect.

The results of the experiments [1] show, however, that this effect is ineffective. That is, the damping due to the large assembly of the B spins is not influenced by the pulses and is given (in our notation) by decay rate Γ_0 which is supposedly a characteristic of the SD mechanism. So, the intensity-dependent damping can be related only to the excited spins themselves. Experiments of [1] and, in particular, the dependence of Γ on Θ_2 show that the 'active' spins do not have the resulting disturbing moment which affects these spins and, hence, do not contribute to the echo decay. On the other hand, it is clear that the local fields of the 'passive' spins at the sites of the 'active' spins have such nonzero moments which leads to the echo decay. It is clear also that this decay rate depends on the amplitude of the transverse (u, v) components of the 'passive' spins, that is on the excitation field. Since the decay rate is constant during the free evolution (for $\tau \ll T_1$) while $u(t)$ and $v(t)$ are oscillatory even in RRF

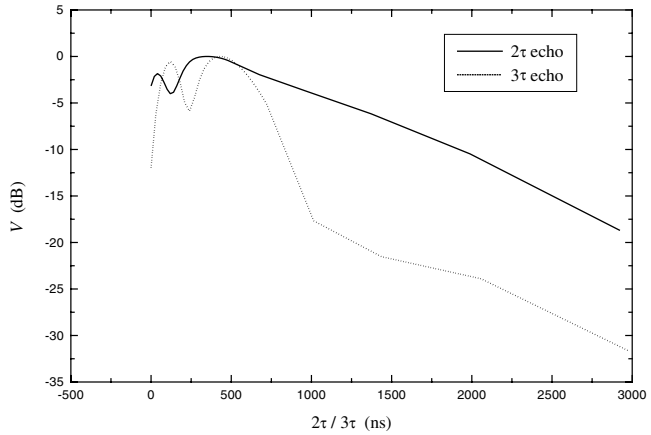

Figure 8. The decay behaviour of the first echo $V(2\tau)$ (full curve) and of the second echo $V(3\tau)$ (dotted curve). For the parameters see the text.

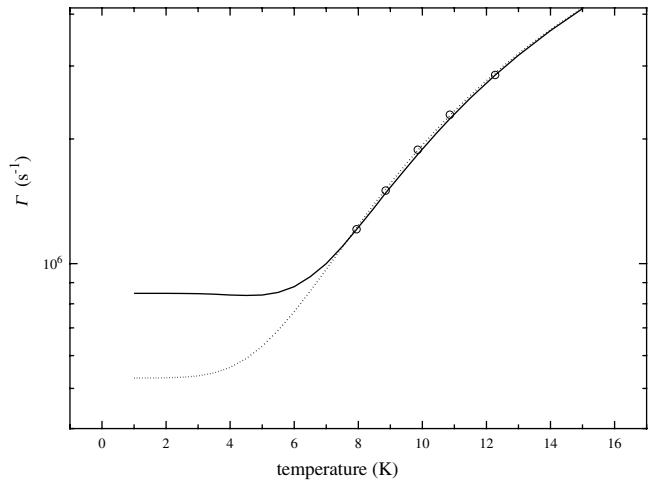

Figure 9. Temperature dependence of the first echo decay rate Γ. Circles are the measured decay rate [2], the full curve depicts the calculated Γ and the dotted curve is Γ_{eff} (equation (24)).

(for $\varepsilon \neq 0$), the decay rate is expressed through the change of the longitudinal component of the Bloch vector $w(t)$: $\Gamma \sim w_0 - \langle w_{pas}(t_2)\rangle$, as follows from the experiment [1].

The decay rate after the second pulse $\Gamma(2)$ in [1] and here is given by one and the same expression (15). However, the physical meaning of the damping mechanism as described in [1] is essentially different from that given in sections 2 and 3 and above in this section. In [1] there is no discrimination between the 'active' and 'passive' spins excited by the second pulse and $\langle w(t_2)\rangle$ in the expression for $\delta w(t_2)$ intuitively implies the average over the inhomogeneous distribution of the polarization of the 'active' spins (in our terminology above). In the present paper, this decay is caused by the 'passive' spins excited during the second pulse.

We hope that some light was shed by the results of sections 2 and 3 and the present discussion on the understanding of the ID and SD mechanisms.

Unlike the ineffective ID effect, there is another one also initiated by the excitation pulses and in this sense 'instantaneous', which we shall term an active spin frequency modulation

(ASFM) effect. It is caused by the 'active' spins and described by the expressions for ϖ_k in (10) and for $\delta\omega^{(2)}$ in (19). In distinction from the incoherent ID effect, the ASFM effect is a consequence of the successive action of the two excitation pulses. The main feature of this effect is that it directly connects the frequency unbalance of a kth 'active' spin with the well defined phase properties of the same kth spin. As shown above, this effect represents the new nonlinear mechanism of the multiple echo formation, the intensity-dependent dispersion mechanism.

We have also shown how the distribution of the resonance frequency influences (negatively) the formation of the multiple echoes.

The results of sections 2 and 3 permit us to obtain further insight into the time decay of the TN and FID [5, 6, 11]. The important statement in [11] is that the power-dependent decay of TN and/or FID is caused by the interaction of the generic coherently excited spin with the fields of other also coherently excited spins. This statement is the opposite to that in the previous publications where the non-Bloch (power-dependent) behaviour has been ascribed to the fluctuations of the resonance frequency of the active centres and/or of the field source.

The arguments about the properties of the '*active*' and '*passive*' spins remain valid also for TN and FID. The TN process consists of the many decaying Rabi oscillations during which the mw field excites the spins of the very different mutual phases; as a consequence, we again have the nonzero local fields and the power-dependent decay. The above is operative for the steady-state prepared FID as well. Of course, such peculiarity as the different role of T_{2u} in TN and in FID [11] remains in force.

Already it has been said in the introduction and confirmed by the calculations that it is more correct to refer the power-dependent damping of the echo to the changes in the longitudinal component of the magnetization than to its transverse components. This conclusion, apparently, is valid for TN and FID. It is pertinent to say that TN, FID and hole burning are less subtle processes than the echo as they do not contain the division to active and passive spins with their subtle dispersion and damping properties and the phase reversal important for echoes. In particular, the FID decay is described by the power-dependent decay rate Γ_{2v} which is constant during the decay process without respect to whether it caused by the changes in the longitudinal component or in the transverse components. To show that the FID is correctly described by equation (15) of [11], if $\Gamma_{2v} = T_{2v}^{-1}(\chi)$ is defined by equation (15) in this paper where $\delta w(t_2) = w_0 - \langle w(t_2)\rangle$ and $\langle w(t_2)\rangle$ is the average polarization at the end of the steady-state preparation, we have recalculated the Rabi frequency dependence of the FID rate. The result is shown in figure 10 by the open diamonds together with the previous calculated result [11] (open circles) obtained with Γ_{2v} expressed through the transverse components of the Bloch vector. There is good agreement between the present result, the previous one and that obtained experimentally by Boscaino and La Bella [5] (solid triangles). The theoretical results for the FID rate [5, 7] following from the OBE (solid squares) and from the Redfield theory (solid circles) are also shown in the figure. In obtaining this result, the following values of parameters from [11] were used (compare with those in [11] where the average of the transverse components is defined in a different way than in (17) and (19) above): $a_\omega = 5 \times 10^7$ cm^{-3} s^{-1}, $a_\Gamma = 3.8 \times 10^7$ cm^{-3} s^{-1}, $r^2 = 1 \times 10^{-8}$ s^2 and $\sigma = 2\pi \times 0.25$ MHz with the same values of T_1 and T_2 as given in [11].

5.2. *High field ESEs*

Previous theories of ESEs in solids cannot explain the existence of the multiple echoes at high applied fields, as it does the present theory. Since the multiple echoes are due to the ASFM effect, they permit us to estimate the nonlinear dispersion parameter a_ω^{ac}, that is

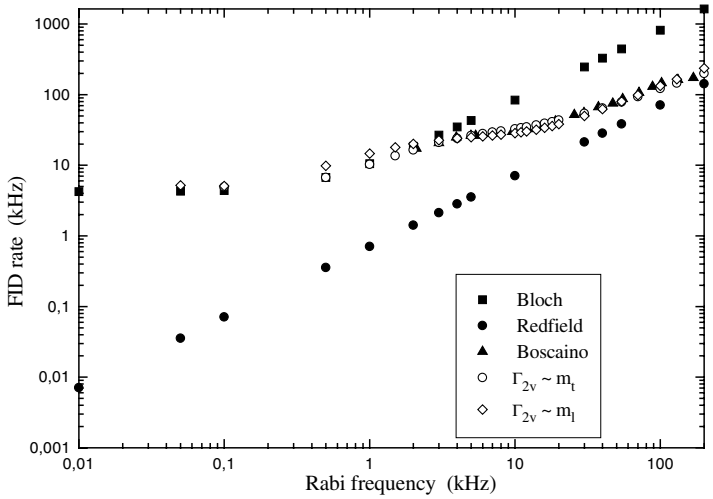

Figure 10. Calculated FID rate, $\Gamma/2\pi$, versus Rabi frequency, $\chi/2\pi$, for sample no 1 of [5]: open circles and open diamonds are for Γ_{2v} expressed through the transverse [11] and longitudinal components (present work) of the Bloch vector respectively. Solid triangles are experimental data of Boscaino and La Bella [5]. Solid squares and solid circles are the theoretical dependences expected from the OBE theory [5] and from the Redfield theory [7] respectively.

the demagnetizing field in the sample. Hence, the echoes depend on the sample form and orientation relative to the applied field.

Due to the ASFM effect, the echo decay is not exponential as is seen from figure 8. In terms of the Bessel functions $J_n(x_1)$, $J_m(x_2)$, the echoes are described by the complicated expression containing the sum over n, m of products $J_n(x_1)J_m(x_2)$. At times $\tau \leqslant T_2$, where $|x_1| > 1$ and $|x_2| > 1$, the τ-dependence of the echoes is governed by the oscillatory behaviour of the Bessel functions. For $\tau \gg T_2$ one has $x_{1,2} \ll 1$ and $V(2\tau) \sim J_1(x_1)J_0(x_2) \sim x_1 \sim \exp(-2\tau/T_2)$, that is an exponential decay for large τ. Note that the nonexponential decay is characteristic for any echoes with significant contribution from the intensity-dependent dispersion and/or damping [4, 20, 21, 24]. We hope that the theory described in sections 2 and 3 can help in further experiments on the high field echoes and their explanation.

5.3. Photon echoes in solids

Several important properties of the photon echoes in solids are similar to those of the ESEs: both cases need the applied magnetic field, have approximately the same memory decay rates, which decrease with increasing field [2, 25] if spin–spin interactions control the dephasing, and so on. The intensity-dependent frequency shift and decay rates for photon echoes in solids were observed [8–10] and ascribed to the ID mechanism through the magnetic dipole–dipole interactions of the active centres [9] In these and in other following publications, however, the conclusion about the power-dependent decay rate is again deduced, as in [1], from the averaging of the polarization of the '*active*' centres.

In our opinion, the division of the centres excited by the second light pulse into the 'active' and 'passive' ones is correct for the photon echoes as well; the power-dependent decay rate of the photon echoes in solids is then caused by the spin polarization of the 'passive' centres while the 'active' centres serve as the origin of the nonlinear mechanism for multiple photon echoes.

6. Conclusion

It is well known that the OBEs with power-independent relaxation and tuning parameters fail to explain ESEs in solids. We presented a modified version of the Bloch equations (MBEs) with specific power-dependent relaxation and dispersion parameters characteristic for two-pulse excitation and when the magnetic dipole–dipole interactions in the system control the dephasing. We have found that the first and second pulses vary the parameters in different ways, so the free evolution of the spins between the pulses and after the second pulse is governed by MBEs with essentially different parameters.

A crucial point here is the division of the spins excited by the second pulse into the 'active' (excited by both pulses and forming the echo signals) and 'passive' (excited by the second pulse only) ones with their essentially different contributions to the power-dependent relaxation and dispersion. It is shown that the 'active' spins participate in a new effect, an ASFM effect giving rise to the power-dependent dispersion and multiple ESEs; the 'passive' spins contribute to the power-dependent relaxation.

These equations are solved and a general expression for the two-pulse ESEs is obtained. Detailed numerical analysis of this expression gives results in good quantitative agreement with the recent experiments [1] on the two-pulse ESEs at conventional low applied fields. From the experiments [1] on the echo decay it is found that the ID effect [3] is ineffective. Also, the developed theory is applied successfully to multiple ESEs at high fields, which are promising for future investigations [2].

Acknowledgments

The authors would like to thank the referees for critically reading the article and useful comments.

References

[1] Agnello S, Boscaino R, Cannas M and Gelardi F M 2001 *Phys. Rev.* B **64** 174423
[2] Kutter C, Moll H P, van Tol J, Zuckerman H, Maan J C and Wyder P 1995 *Phys. Rev. Lett.* **50** 1269
[3] Klauder J R and Anderson P W 1962 *Phys. Rev.* **125** 912
[4] Deville G, Bernier M and Delrieux J M 1979 *Phys. Rev.* B **19** 5666
[5] Boscaino R and La Bella M V 1990 *Phys. Rev.* A **41** 5171
[6] Boscaino R, Gelardi F M and Korb J P 1993 *Phys. Rev.* B **48** 7077
[7] De Voe R G and Brewer R G 1983 *Phys. Rev. Lett.* **50** 1269
[8] Huang J, Zhang J M, Lezama A and Mossberg T W 1989 *Phys. Rev. Lett.* **63** 78
[9] Liu G K and Cone R L 1990 *Phys. Rev.* B **41** 6193
[10] Kroll S, Xu E Y, Kim M K, Mitsunaga M and Kachru R 1990 *Phys. Rev.* B **41** 11568
[11] Asadullina N Ya, Asadullin T Ya and Asadullin Ya Ya 2001 *J. Phys.: Condens. Matter* **13** 3475
[12] Asadullina N Ya, Asadullin T Ya and Asadullin Ya Ya 2001 *J. Phys.: Condens. Matter* **13** 5231
[13] Shakhmuratov R N, Gelardi F M and Cannas M 1997 *Proc. SPIE* **3239** 206
[14] Shakhmuratov R N and Khasanshin R A 1997 *Proc. SPIE* **3239** 357
[15] Wodkiewicz K and Eberly J H 1985 *Phys. Rev.* A **32** 992
[16] Berman P R and Brewer R G 1985 *Phys. Rev.* A **32** 2784
[17] Malinovsky V S and Szabo A 1997 *Phys. Rev.* A **55** 3826
[18] Redfield A G 1955 *Phys. Rev.* **98** 1787
[19] Tomita K 1958 *Prog. Theor. Phys.* **19** 541
[20] Fossheim K, Kajimura K, Kazyaka T G, Melcher R L and Shiren N S 1978 *Phys. Rev.* B **17** 964
[21] Asadullin T Ya and Asadullin Ya Ya 1997 *J. Phys.: Condens. Matter* **9** 9361
[22] Altshuler S A, Kurkin I N and Shlyonkin V I 1980 *Zh. Eksp. Teor. Fiz.* **79** 1591
[23] Asadullin Ya Ya 1993 *J. Phys.: Condens. Matter* **5** 3689
[24] Gould R W 1969 *Am. J. Phys.* **37** 585
[25] Ganem J, Wang Y P, Meltzer R S and Yen W M 1991 *Phys. Rev.* B **43** 8599